# A double-digitising method for building 3D virtual trees with non-planar leaves: application to the morphology and light-capture properties of young beech trees (Fagus sylvatica)

Jean-Christophe J.-C. Chambelland, M. Dassot, A. Adam, N. Donès, Philippe Balandier, A. Marquier, M. Saudreau, G. Sonohat, Hervé Sinoquet

doi : 10.1071/FP08051

Functional plant biology, vol. 35, 2008, p. 1059-1069

**Title**: A double-digitizing method for building 3D virtual trees with non-planar leaves – application to the morphology and light capture properties of young beech trees (*Fagus sylvatica*).

**Authors**: Jean-Christophe Chambelland[A], Mathieu Dassot[A], Boris Adam[A], Nicolas Donès[A], Philippe Balandier[AB], André Marquier[A], Marc Saudreau[A], Gabriela Sonohat[AC], Hervé Sinoquet[AD]

**Addresses**:

[A] UMR547 PIAF, INRA, UNIV BLAISE PASCAL, 234 Avenue du Brézet, F-63100 CLERMONT FERRAND, France

[B] Cemagref, UR EFNO, Domaine des Barres, F-45290 Nogent-sur-Vernisson, France

[C] ENITAC, Site de Marmilhat, BP35, F-63370 LEMPDES, France

[D] Corresponding author. Email: sinoquet@clermont.inra.fr

Number of words: 6142 (Abstract to references)

Abstract: 185

Number of tables: 2

Number of figures: 10

doi : 10.1071/FP08051


## Abstract

We developed a double-digitizing method combining a hand-held electromagnetic digitizer and a non-contact three-dimensional (3D) laser scanner. The former was used to record the positions of all leaves in a tree and orientation angles of their lamina. The latter served to obtain the morphology of leaves sampled in the tree. As the scanner outputs a cloud of points, software was developed to reconstruct non-planar (NP) leaves composed of triangles, and to compute numerical shape parameters: midrib curvature, torsion and transversal curvature of the lamina. Combination of both methods allowed building 3D virtual trees with NP leaves.

The method was applied to young beech trees (*Fagus sylvatica*) selected in different sunlight environments (from 1 to 100% of incident light) in forest of central France. Leaf morphology responded to light availability, with more bent shape in well lit leaves. Light interception at the leaf scale by NP leaves was decreased from 4 to 10%, for shaded and sunlit leaves compared to planar leaves. At the tree scale, light interception by trees made of NP leaves was decreased by 1 to 3% for 100% to 1% light, respectively.


**Keywords:** Virtual plants, laser scanner, electromagnetic digitizing

doi : 10.1071/FP08051

## Introduction

Most trees have a strong ability for structural modification in response to light availability. At the plant scale, leaf distribution has been reported to be more regular and more clumped in shaded and sunny environments, respectively (Planchais and Sinoquet 1998; Farque *et al.* 2001). Leaf attributes may also change, e.g. inclination and rolling angles of the whole lamina show significant changes with regard to irradiance level (Begg 1980; Niklas and Owens 1989; Heckathorn and DeLucia 1991; Midgley *et al.* 1992; Planchais and Sinoquet 1998). For example, in a recent study on *Fagus sylvatica* data showed that leaf number, mean leaf angle and leaf dry matter content per unit area increased with light availability (Balandier et al. 2007). In addition, several species may show structural changes affecting the leaf morphology, such as lamina folding or curling (Innes 1992; Muraoka *et al.* 1998; Fleck *et al.* 2003; Niinemets 2007). These multiple ways for changing the tree geometry has consequences for the plant's ability to intercept light, and usually allows plants to maximize light capture in low light and protect themselves against photo inhibition of photosynthesis in excess light (Pearcy *et al.* 2005).

Three-dimensional (3D) virtual tree modelling (Prusinkiewicz and Lindenmayer 1990; Weber and Penn 1995; Lintermann and Deussen 1998, Godin and Sinoquet 2005) has become a promising tool for quantifying structural responses in relation with both the geometry and the spatial distribution of the tree organs. In combination with radiation transfer models or foliage projection model, the quantification of light interception at tree scale has been widely addressed using virtual tree mock-ups constructed from measurements (e.g. Sinoquet and Rivet 1997, Sinoquet *et al.* 1998, Sonohat *et al.* 2006). Measurements are presently considered to be the most accurate approach to quantitatively represent the 3D tree architecture, because the actual features of tree geometry are taken into account. These processes are typically composed of two steps: an acquisition step consisting of capturing the

geometrical features of the tree organs using a suitable digitizing device (e.g. Hanan and Room 2002), and a reconstruction step in which the resulting data are converted to a suitable 3D computer mock-up.

Hand-held electromagnetic digitizers (HHEMD) provide a robust way for quantifying the tree geometry in a systematic manner especially the capture of the spatial position and orientation of stems and leaves (Sinoquet and Rivet 1997; Sinoquet *et al.* 1998; Sonohat *et al.* 2006). However, HHEMD are tedious, time-consuming and often not enough precise for accurately capture the detailed leaf geometry, e.g. measuring the leaf edges (see Rakocevic *et al.* 2000 for white clover digitizing). This is the reason why most plant mock-ups constructed from HHEMD do not integrate the non-planar (NP) leaf structure. Indeed leaf shape is often reduced to planar polygons, *de facto* neglecting a potential influence of leaf curvature or leaf torsion on the whole-plant light interception.

Conversely, other emerging 3D capture devices such as non-contact laser scan digitizers (NCLSD) have been used for various plant measurement and reconstruction (e.g. Tanaka *et al.* 1998; Kaminuma 2004; Rice *et al.* 2005; Dornbusch *et al.* 2007). Indeed, NCLSD are able to rapidly quantify the surface of an object under investigation as a dense set of points and consequently they seem potentially useful for modelling 3D virtual trees at a fine scale. A drawback of this type of device is that organs that are overlaid are not "viewed" by the scanner, e.g. a twig under a leaf, and thus not considered. Other drawback is the segmentation task which is needed to clearly distinguish subsets of points related to the plant organs such as leaves and stems. In practice automatic segmentation remains an open problem due to holes, spikes, hidden parts, and data points that do not belong to the scanned tree (Hanan *et al.* 2004). Therefore the segmentation task must in most cases be manually achieved (Dornbusch *et al.* 2007) through numerous fastidious interactive manipulations.

The present work was an attempt to combine the advantages of HHEMD and NCLSD for building 3D virtual trees composed by NP leaves. In this goal, a four-step reconstruction protocol was investigated: i) a 3Space Fastrack Polhemus HHEMD ( www.polhemus.com ) was used to describe the location and orientation of all leaves in the tree, and the maximum width and length of each leaf was manually measured with a ruler; ii) a Konica VIVID 910 NCLSD ( www.konicaminolta.com ) was used for capturing the geometry of a sample of leaves leading for each digitized leaf to a dense set of 3D points; iii) each set of leaf points was processed to extract numerical parameters featuring the leaf 3D morphology, and derive a normalized triangulated leaf model by fitting a set of triangles onto the 3D leaf data points; iv) the HHEMD data were combined with the triangulated leaves in order to get 3D tree mock-ups with NP leaves. This framework was applied on young European beech trees (*Fagus sylvatica*) selected in different sunlight environments in forest in central France, in order to investigate how morphological leaf parameters change with light availability and the consequences on light capture ability.

## Material and methods

### *Tree selection in a light gradient*

Eleven young beech trees were selected in the Chaîne des Puys, a mid-elevation volcanic mountain range situated in the Auvergne region of France (45°42' N, 2°58' E). All trees except one were located in a forest dominated by *Pinus sylvestris*. Light availability for each sapling was estimated as follows. A digital fisheye camera fixed in a self-levelling device was positioned just above the sapling, with the camera objective perpendicular to the soil surface. The camera was connected to a PC for real-time photograph segmentation into sky and vegetation pixels, and for analysis of light availability in percent of above canopy value (%light) with software PiafPhotem (Adam *et al.* 2006). The trees were chosen in the range of

111 %light between 1 and 100%, i.e. from the limit of beech growth in the very shade to open
112 area. Trees were separated in four light classes (Table 1). Beech height ranged between 0.4
113 and 1.1 m, and included between 110 and 3400 leaves.

114

115 *Tree mock-up reconstruction process*

116 We only considered leaves in this study. While petioles and branches participate to the
117 modification of canopy architecture and thus, indirectly, to light interception, leaf distribution
118 in space takes into account these features and the time for digitizing the tree (see below) is
119 accordingly reduced. A four-step 3D tree mock-up reconstruction method was developed.
120 First, the HHEMD was used to measure all leaf positions and orientation angles of each tree,
121 and the maximum width and length of each leaf was manually measured with ruler. This step
122 was realised in a non-destructive manner, by digitalizing and measuring the trees directly in
123 their natural environment. Second, 3D laser scans of nine individual leaves per tree (three
124 leaves in each of the lower, middle and upper part of the tree) were produced with the
125 NCLSD. The scans were realised on freshly harvested leaves which were transported (in
126 about one hour of travel) in plastic bag from the Chaîne des Puys to a scanning lab. Third,
127 each set of 3D scanner leaf points was computer processed to extract leaf shape parameters
128 and to produce a normalized triangulated leaf model. Fourth, the triangulated leaf models
129 were positioned in the tree structure according to leaf positions, orientations and dimensions
130 measured in step one.

131

132 *HHEMD for capturing leaf position and orientation (first step)*

133 A 3Space Fastrack Polhemus HHEMD ( www.polhemus.com ) was used to digitize all leaves
134 in each selected tree. This device is composed of a transmitter and a receiver connected to a

central unit. Both the transmitter and receiver contain a triad of electromagnetic coils. Those in the transmitter are supplied with alternating voltage, so that they emit alternating magnetic fields. When located in the magnetic fields, coils in the receiver show induced currents, the value of them is related to the location and orientation of the receiver with regard to the transmitter (Polhemus Inc. 1993). In practice, the transmitter must be placed near the target tree for defining a global 3D Cartesian reference system **(O, X, Y, Z)**. The receiver is inlayed into a handle which allows an operator collecting/picking 3D points on the plant. The accuracy of the device allows an approximate capture resolution of 0.8mm in a volume depending on the magnetic source, here up to 3 m around the transmitter but acquisition is possible up to 9 m with a more powerful transmitter. Each measurement produces 6 data, namely a triplet of Cartesian coordinates locating the digitized point in the global reference system, and the receiver orientation provided as Euler angle triplet i.e. azimuth, elevation and roll angles. Data acquisition is driven by software PiafDigit (Donès *et al.* 2006) available at http://www2.clermont.inra.fr/piaf/eng/download/download.php .

For leaf digitizing, the receiver was pointed at the proximal point of the lamina (i.e. the junction between petiole and lamina) and oriented parallel to the midrib and to the mean plane of the lamina (Fig. 1a). The receiver inclination was visually approximated by the leaf axis, i.e. the line between the proximal and distal points of the midrib. With this orientation, the Euler angles were the midrib azimuth, the midrib inclination and the roll angle of lamina around the midrib (Sinoquet *et al.* 1998). During digitizing, leaf length and maximum leaf width along the midrib were manually measured with a ruler, and the data were input in the same software PiafDigit. The output of the HHEMD measurements was an ASCII file per tree. Each file contained the list of tree leaves with their maximum width and length, orientation angles and spatial coordinates. The related tree mock-ups with planar leaves were

visualized with the software VegeSTAR also available at http://www2.clermont.inra.fr/piaf/eng/download/download.php (Adam *et al.* 2002) (Fig. 2a).

*NCLSD for capturing the leaf geometry (second step)*

A Konica Minolta VIVID 910 NCLSD ( www.konicaminolta.com ) was used to capture the leaf geometry. This device is composed of a single parallelepiped unit presenting two circular apertures hosting a laser emitting unit and a charge-coupled device (CCD) camera, respectively (Fig. 1b).

The VIVID 910 uses a light-stripe method to acquire object geometry. This technique (Fig. 3) consists of emitting a horizontal red laser ray through a cylindrical lens to the object and to convert the reflected light into distance information by using an active triangulation principle. The conversion is achieved through the CCD (here a 640*480 pixels) camera. The process is repeated by scanning the light stripe vertically on the object surface using a rotating mirror. The result is a dense set of 3D points outlining the part of the object which is visible for the CCD. The VIVID 910 is provided with three interchangeable receiving lenses allowing an angular field of view approximately covering 10 $cm^2$ to 1 $m^2$. The recommended scan distance is between 0.6 m and 2.5 m and the scanner resolution, i.e. the distance between two digitized points, varies from 0.039 mm to 0.090 mm according to the lens. An efficient embedded auto focus technology allows automatically detection of the optimal scan distance for a given lens and a given object. The number of digitized points varies with two resolution modes and the ratio between the object size and the CCD field of view. In addition, a 24-bit colour image is captured at the same time by the CCD camera. For our study, the VIVID 910 was driven from the commercial software rapidform2006 (INUS Technology, Seoul, Korea). This industrial software is widely used for computer-aided design issues, and provides a comprehensive suite

of tools designed to process real-world data, from 3D scanning devices control to parametric surface reconstruction.

The smallest lens with the fine resolution mode (0.039 mm) was used for capturing the geometry of 99 leaves, i.e. 9 leaves per beech tree. Three leaves were harvested in each of the lower, middle and upper part of the tree. Each of the 99 leaves was positioned in front of the VIVID so that the CCD camera viewed maximum projected area of the leaf (Fig. 1b). The VIVID was levelled and the leaf axis was set vertically, i.e. parallel to the VIVID Y-axis. Identification of the leaf axis in both the HHEMD and NCLSD data ensured the geometric consistency between 3D data at tree and leaf scales. During our measurements, we overcame segmentation problem related to the use of NCLSD since all digitised points belonged to the scanned leaf. Each 3D digitized leaf included between 10,000 and 30,000 points depending on leaf size. An image of the 3D data points for a digitized medium-sized leaf is given in Fig. 4a.

### L*eaf shape parameter extraction and leaf triangulation in 3D (third step)*

Three-dimensional data obtained from the NCLSD for each leaf were processed for both extracting a set of numerical parameters featuring the leaf morphology and for constructing a non-planar triangulated model of each harvested leaf. An application programming interface which allows direct access to data structures and algorithms in rapidform2006 via the Microsoft Visual C++ programming language was used to develop a rapidform2006 plug-in. Extracted morphological parameters were midrib length L (mm), maximum leaf width W (mm), leaf area A ($mm^2$), midrib curvature C ($mm^{-1}$), openness angle between two half-laminas O (°), lamina twirl T (°), transversal curvature angle of lamina TC (°) and symmetry between the two half-laminas S, i.e. the ratio of the left leaf half width to the total leaf width along its midrib. The extraction algorithm was based on a set of slicing free form NURBS curves (Piegl and Tiller 1997) equidistantly subdividing the leaf along its midrib (Fig. 4b). The set of 3D points for each leaf was transformed into an oriented set of curves: one curve

for modelling the midrib, and n curves for modelling the transversal shape of the lamina (Fig. 4b). The shape parameters were then extracted from the length and the curvature of the (n+1) curves. The mean, minimal and maximal values of the shape parameters were computed for each leaf from the values of the (n+1) curves. Additional parameters were computed from A, L and W, namely the ratio W/L, and the allometric coefficient K defined as the ration between A and the product L W. One can notice the difference between the quantification of the midrib curvature, expressed in $mm^{-1}$, and the quantification of the transversal curvatures, expressed in degrees (°). The former is the mathematical differential curvature of the midrib curve, i.e the inverse of the radius of the osculating circle (Piegl and Tiller 1997; Fig. 5). This curvature has been proved efficient for quantifying the oscillations of the midrib because of its low number of curvature variations. Conversely, practical evidences showed us that the differential curvature was not a good solution for measuring the curvature of the transversal NURBS curves because of their high number of local variations, often leading to null or enormous curvature. For this reason, we preferred to measure the transversal curvature of the leaf using an angle, which can be interpreted as the aperture angle of the half laminas (Fig. 5). The quantity S is a ratio of two lengths which represents the level of symmetry of the leaf along its midrib. This ratio is computed for each slicing curve. It is defined as the ratio between the left half-lamina width (i.e. the length of the slicing curve from le left bound of the leaf until the intersection with the midrib) and the total width of the leaf (i.e. the total length of the slicing curve). S varies from 0.0 for a very dissymmetric piece of leaf until 0.5 for a perfectly symmetric peace of leaf. Note that the "left" direction is defined by the direction of the negative abscissa (X-) of the coordinate system linked to the laser scanner (Fig 5).

A triangulated model of each leaf composed of 8n triangles was also constructed from the (n+1) curves (Fig. 4c). The triangulated leaves were normalized so that the distance between the proximal and distal point of the lamina in the leaf model was 1. Here n was set to 9, leading to 72 triangles per leaf. This value is a compromise between accuracy in the NP leaf description and file size. Morphological parameters were exported to Microsoft Excel files while the triangulated leaves were converted in VegeSTAR format as a set of triangles for further visualization and light interception computation. We verified that the leaf surface covered by the digitized points was equivalent to the one given by the triangulated leaf model in VegeSTAR ($R^2$ = 0.98 with a 2% error between values given by the digitized and the triangulated leaves).

*Replacing the planar hexagonal leaves by non-planar triangulated leaves (fourth step)*

A specific computer program was developed for replacing the planar hexagonal leaves by the NP triangulated leaves in the eleven tree mock-ups built from the HHEMD. For each planar leaf in the tree, a normalized triangulated leaf model was randomly selected among those owning to the same layer (upper, medium or lower) in the same tree. In order to support the comparison of planar leaves with NP leaves, the selected normalized triangulated leaf model was then scaled, rotated and translated in the tree structure according to the geometrical attributes of the planar leaf i.e. $L^2$, Euler angle triplet and Cartesian coordinates respectively. The geometry of the 3D trees with NP leaves were saved as VegeSTAR files as a collection of triangles for further visualization (Fig. 2b) and light interception computations.

*Computing light interception at leaf and tree scales*

Three-dimensional mock-ups of both, individual leaves and trees were used in software VegeSTAR for light interception computations (Adam *et al.* 2002). In the software, the 3D scene elements are geometrical primitives assigned with false colours. The principle of VegeSTAR consists of taking a picture of the 3D scene from the sun (or any other light source) direction Ω with a virtual orthographic camera (Sinoquet *et al.* 1998). The scene elements seen on the picture are those lit from the view direction. The amount of projected area intercepting light in direction Ω is then estimated from the coloured pixel counts in the image. Light interception is finally characterized by the variable STAR (Silhouette to Total Area Ratio; Carter and Smith 1985; Oker-blom and Smolander 1988), which is the ratio between the projected area seen on the image and the total area contained in the scene. As STAR depends on the incident direction Ω, the sky hemisphere was divided in 46 solid angle sectors of equal measure, according to the Turtle sky proposed by Den Dulk (1989). Directional STAR values were computed for the central direction of each solid angle sector. Directional STAR values then were summed up over the sky hemisphere after weighting with coefficients derived from the Standard OverCast distribution of sky radiance (Moon and Spencer 1942). The resulting value $STAR_{SKY}$ characterized light interception over the sky vault. Both directional and hemispherical STAR values were computed at the individual leaf scale for the 99 laser-scanned leaves displayed with horizontal leaf axis and null whole lamina rolling. STAR values were also computed at the tree scale with planar leaves and NP leaves, i.e. taking into account the size, orientation and location of each leaf in the tree. The use of the STAR at tree level as an indicator of light interception efficiency was previously validated for beech (Balandier et al. 2007); diameter growth (or biomass increment) of young beeches was related to the combination of STAR, leaf area, and available light above the young beeches with a good accuracy ($r^2 = 0.86$ ; $p < 0.0001$).

### *Statistical data analysis*

The analysis of variance of leaf parameters (table 2) was determined using a mixed general linear model, with the mixed procedure (Proc Mixed) in SAS version 8.2 (Christophe et al. 2006). The effects of individual plants were added as random effects in the error of the model, using the repeated option in Proc Mixed. The variance–covariance matrix of the error was specified by an autoregressive model. When data were analysed by regression (figures 7 to 10) differences in the slopes between different light classes were tested with an F test after linearization if necessary.

## Results

### *Leaf morphology*

The leaf morphology depended on the light available above the plant. Shaded plants were almost flat becoming more bent when exposed to increased light above the plant (Fig. 6). A quantitative analysis of the leaf morphology parameters showed a significant effect of %light on the following parameters (Table 2): minimal openness angle between the two half-laminas ($O_{min}$), maximal lamina twirl angle around the midrib ($T_{max}$), minimal transversal curvature angle ($TC_{min}$), and allometric coefficient K. Midrib curvature C did not show any significant change with %light, although it would contribute to strengthen the bent aspect of leaves. The higher value of K in full light meant that the same leaf area was achieved with smaller leaf length and leaf width (no significant change was found in the ratio W/L).

### *Light interception at leaf scale*

A linear regression analysis between individual leaf area and its projection averaged over all sky directions showed differences in light capture efficiency according to %light (Fig. 7;

slopes were statistically different at $P < 0.0001$). Higher light led to lower $STAR_{SKY}$, with slope values of 0.96-0.97, 0.94 and 0.90 for plant irradiance between 1-15%, 30-40% and 100%, respectively. For any light class, $STAR_{SKY}$ values only showed little variations with leaf size, since the coefficient $R^2$ was always very high.

Directional STAR values showed high variation with the elevation angle h of the incident beam direction (Fig. 8). The main source of variation was the angle between the beam direction and the leaf normal, as directional STAR of a horizontal planar leaf is defined by the sine function *sin*(h), i.e. STAR ranging from 0 to 1 for h between 0 and 90°. However, directional STAR values of NP leaves showed some deviations with regard to that of a planar leaf. For low elevation angles (h<20°), STAR values of NP leaves was slightly higher than that of planar leaves, while STAR of NP leaves was lesser than that of planar leaves for h>20°. The magnitude of the deviation for both low and high elevation angles was related to %light, with greater deviations for more lighted plants (Fig. 8; $P = 0.009$).

### *Light interception at tree scale*

$STAR_{SKY}$ values of the whole trees with NP leaves were also lower than those of trees with planar leaves (Fig. 9; slope of the regression line statistically different from the 1:1 line at $P < 0.0001$). In contrast with the leaf scale, the tree $STAR_{SKY}$ decrease when tree was built with NP leaves did not depend on %light, and the magnitude of STAR reduction was a maximum of 3.2% for all light classes. Moreover the higher %light, the lower STAR value, leading to a smaller effect of NP leaves on the absolute $STAR_{SKY}$ value at tree scale.

For %light below 40%, tree directional STAR increased with elevation angle (Fig. 10). For low elevation angles, trees with %light below 40% showed similar values of directional STAR around 0.21 without any differences between trees with planar leaves and trees with

NP leaves. For elevation angles above 20°, differences in directional STAR between %light classes increased with elevation angles (slopes of the regression line after linearization statistically different between %light classes at $P < 0.0001$), with higher STAR values for the more shaded plants (Fig. 10). For that elevation angles higher than 20° STAR of trees with NP leaves was always slightly lower than that of trees with planar leaves, with the maximum differences being around 45-50° of elevation. The tree in full light showed a particular behaviour with a small bell shaped curve of directional STAR with elevation and only a very slight decrease in case of trees with NP leaves.

doi : 10.1071/FP08051

## Discussion

### *A double-digitizing method for 3D plant structure*

We developed a double-digitizing method to build 3D plants with non-planar leaves (NP leaves). Indeed only one digitizing method would be insufficient for this purpose. Contact digitizers (e.g. hand-held electromagnetic digitizer, HHEMD, used here) are not accurate enough and only allow a rough description of the 3D leaf shape (e.g. Rakocevic et al. 2000). Non-contact laser scan digitizers (NCLSD) are better suited for continuous surfaces (i.e. their current use in industrial applications) than for plants where many small surfaces are distributed in the vegetation volume. This is the reason why laser scanner applications to building 3D plants deal with simple isolated plants with a few organs (Kaminuma et al. 2004; barley, Dornbush et al. 2007) or isolated leaves (Loch 2004). The scan of a leaf is easy and very rapid (less than 1 minute) in the lab where focus is easy to do with controlled light conditions. The scan could be more complicated with *in situ* organs in the field conditions with organs moved by the wind and none controlled light conditions leading to many artefacts in the point cloud. Scanning in the field would obviously require plant protection, at least from wind and light.

Scanner application to more complex whole plants is presently limited by the segmentation of the 3D data set, as suitable automatic algorithms are for the moment unavailable. Moreover scanner beams only hit the plant organs making the plant hull, preventing one to get information inside the plant volume. This problem is emphasized in plants with high foliage density. Dutilleul et al. (2008) used a computed-tomography (CT) scanner to get a full description of the whole plant as a set of 3D data points, i.e. solving the masking effect. This is a great improvement but this is limited to small plants (i.e. able to be inserted within the CT

scanner). Moreover algorithms for the segmentation of the 3D data points, i.e. point assignation to plant organs, are also unavailable.

In consequence, the combination of HHEMD and NCLSD with suitable software turns out to be a reliable approach for rapidly acquiring detailed plant architecture data. A constant problem with such approaches is the validation of the built mock-up, and particularly of the light intercepting surface, i.e. leaf area. What could be a method of reference to measure leaf area, particularly for NP leaves? A flat-bed scanner is probably no more accurate that the scanner laser and in case of discrepancy between both measurements it would be difficult to say which is the "true" leaf area. The same problem is true at the tree scale. It was already assessed by example by Drouet (2003) who compared direct measurements of maize architecture with a 3D-digitization technique. The conclusion was that both techniques were effective; the question is more linked to which resolution we want the spatial data.

### *Effect of light availability on the leaf morphology and consequences on light capture ability*

Non-planar leaf morphology is significantly dependent on light availability, with flatter leaves in shaded environment. This is in agreement with the only study we found on this topic for broad-leaves species (Fleck et al. 2003). In this previous study, the 3D leaf shape was characterised by the average cross-sectional angle between the leaf halves, which was derived from manual measurements. This angle is similar to the openness angle O used in the present study. For beech leaves, Fleck et al. (2003) found a larger range in openness angles, i.e. 170° to 90-100° for shaded and full lit leaves, respectively. Of course, using the laser scanner method allowed us a more detailed characterization of the 3D leaf shape, showing that several parameters accounting for the 3D shape also responded to light availability (Table 2).

Light capture at both leaf and tree scales decreased when the 3D shape of leaves was emphasised, i.e. for higher light availability. This is in agreement with the few previous reported results. At the leaf scale, Fleck et al. (2003) showed lower interception for smaller openness angles between leaf halves, and the decrease in light interception was higher for direct than for diffuse radiation. Our results cannot be directly compared to those of Fleck et al. (2003), because they dealt with direct and diffuse radiation at the daily scale. Rather we showed that differences between planar leaves and NP leaves in directional light interception is low for low elevation angles and markedly increases for higher elevation angles.

At the tree scale, the decrease in hemispherical interception ($STAR_{SKY}$) due to NP leaves was a maximum of 3% mainly for the most shaded beeches (Fig. 9 & 10). The absence of strong differences between light levels might be related to compensation from other structural changes, and among other a higher leaf area density observed in sunny beech plants (e.g. Planchais and Sinoquet 1998; Delagrange et al. 2005). A 3% decrease of light interception at the tree scale may seem relatively low, but this is similar to the effect of other plant processes on carbon acquisition, e.g. the spatial distribution of leaf nitrogen in tree canopies (Hollinger 1996) and heliotropism in cotton crops (Ehleringer and Hammond 1987). The competitive advantage of such a decrease in light interception could be that NP leaves allow better irradiance distribution over the tree leaf area and light penetration into deeper canopy leaves, with positive consequences on the carbon gain by the plant (Niinemets 2007).

## Acknowledgements

This project was funded by INRA, program ECOGER ‘Bases écophysiologiques d’une gestion durable des forêts hétérogènes’ and project PREVOIR funded by the Conseil Régional d’Auvergne.

## References

Adam B, Benoît JC, Balandier P, Marquier A, Sinoquet H (2006) 'PiafPhotem - software to threshold hemispherical photographs. Version 1.0.' (UMR PIAF INRA-UBP: Clermont-Ferrand, France and ALLIANCE VISION: Montélimar, France)

Adam B, Donès N, Sinoquet H (2002) 'VegeSTAR - software to compute light interception and canopy photosynthesis from images of 3D digitised plants. Version 3.0.' (UMR PIAF INRA-UBP: Clermont-Ferrand)

Balandier P, Sinoquet H, Frak E, Giuliani R, Vandame M, Deschamps S, Coll L, Adam B, Prévosto B, Curt T (2007) Six-year evolution of light use efficiency, carbon gain and growth of beech saplings (*Fagus sylvatica* L.) planted under Scots pine (*Pinus sylvestris* L.) shelterwood. *Tree Physiology* **27**, 8, 1073-1082.

Begg JE (1980) Morphological adaptations of leaves to water stress. In 'Adaptation of Plants to Water and High Temperature Stress'. (Eds NC Turner, PJ Kramer) pp. 33–42. (John Wiley: New York)

Carter GA, Smith WK (1985) Influence of shoot structure on light interception and photosynthesis in conifers. *Plant Physiology* **79**, 1038-1043.

Christophe A, Moulia B, Varlet-Grancher C (2006) Quantitative contributions of blue light and PAR to the photocontrol of plant morphogenesis in Trifolium repens (L.). *Journal of Experimental Botany* **57**, 2379-2390.

Delagrange S, Montpied P, Dreyer E, Messier C, Sinoquet H (2006) Does shade improve light interception efficiency? A comparison among seedlings from shade tolerant and intolerant temperate deciduous tree species. *New Phytologist* **172**, 293-304.

Den Dulk JA (1989) 'The interpretation of remote sensing, a feasibility study' PhD Thesis (Wageningen University: Wageningen, The Netherlands)

Donès N, Adam B, Sinoquet H (2006) 'PiafDigit - software to drive a Polhemus Fastrak 3 SPACE 3D digitiser and for the acquisition of plant architecture. Version 1.0.' (UMR PIAF INRA-UBP: Clermont-Ferrand)

Dornbusch T, Wernecke P, Diepenbrock W (2007) A method to extract morphological traits of plant organs from 3D point clouds as a database for an architectural plant model. *Ecological Modelling* **200**, 119-129.

Drouet JL (2003) MODICA and MODANCA: modelling the three-dimensional shoot structure of graminaceous crops from two methods of plant description. *Field Crops Research* **83**, 215-222.

Dutilleul P, Han L, Smith DL (2008) Plant light interception can be explained via computed tomography scanning - Demonstration with pyramidal cedar (Thuja occidentalis, Fastigiata). *Annals of Botany* **101**, 19–23.

Ehleringer JR, Hammond SD (1987) Solar tracking and photosynthesis in cotton leaves. *Agricultural and Forest Meteorology* **39**, 25-35.

Farque L, Sinoquet H, Colin F (2001) Canopy structure and light interception in Quercus petraea (Matt.) Liebl. seedlings in relation to light regime and plant density. *Tree Physiology* **21**, 1257-1267.

Fleck S, Niinemets U, Cescatti A, Tenhunen J (2003) Three-dimensional lamina architecture alters light-harvesting efficiency in Fagus: a leaf-scale analysis. *Tree Physiology* **23**, 577-589.

Godin C (2000) Representing and encoding plant architecture: a review. *Annals of Forest Science* **57,** 413-438.

Godin C, Sinoquet H, (2005) Functional-structural plant modelling. *New Phytologist* **166**, 705-708.

Hanan JS, Loch B, McAleer T (2004) Processing laser scanner data to extract structural information. In: 'Proceedings of the 4th International Workshop on Functional-Structural Plant Models'. (Eds C Godin *et al.*) pp. 9-12. (CIRAD: Montpellier)

Hanan J, Room P (2002) 'Floradig User Manual.' (Centre for Plant Architecture Informatics, University of Queensland: Brisbane, Australia)

Heckathorn SA, DeLucia EH (1991) Effect of leaf rolling on gas exchange and leaf temperature of Andropogon gerardii and Spartina pectinata. *Botanical Gazette* **152**, 263–268.

Hollinger DY (1996) Optimality and nitrogen allocation in a tree canopy. *Tree Physiology* **16**, 627-634.

Innes JL (1992) Observations on the condition of beech Fagus sylvatica L. in Britain in 1990. *Forestry* **65**, 35-60.

Kaminuma E, Heida N, Tsumoto Y, Yamamoto N, Goto N *et al.* (2004) Automatic quantification of morphological traits via three-dimensional measurement of Arabidopsis. *The Plant Journal* **38**, 358–365.

Lintermann B, Deussen O (1998) A modelling method and user interface for creating plants. *Computer Graphics Forum* **17,** 73-82.

Loch (2004) 'Surface fitting for the modelling of plant leaves.' PhD thesis (University of Queensland: Brisbane, Australia)

Midgley GF, Rutherford MC, Davis GW, Bösenberg J de W (1992) Photosynthetic responses of heliophilus Rhus species to environmental modification by invasive shrubs. *Functional Ecology* **6**, 334–345.

Moon P, Spencer DE (1942) Illumination from a non-uniform sky. *Transactions of the Illumination Engineering Society* **37**; 707-726.

Muraoka H, Takenaka A, Tang Y, Koizumi H, Washitani I (1998) Flexible leaf orientations of Arisaema heterophyllum maximize light capture in a forest understorey and avoid excess irradiance at a deforested site. *Annals of Botany* **82**, 297–307.

Niinemets U (2007) Photosynthesis and resource distribution through plant canopies. *Plant, Cell and Environment* **30**, 1052-1071.

Niklas KJ, Owens TG (1989) Physiological and morphological modifications of Plantago major (Plantaginaceae) in response to light conditions. *American Journal of Botany* **76**, 370–382.

Oker-Blom P, Smolander H (1988) The ratio of shoot silhouette area to total needle area in Scots pine. *Forest Science* **34**, 894-906.

Pearcy RW, Muraoka H, Valladares F (2005) Crown architecture in sun and shade environments: assessing function and trade-offs with a three-dimensional simulation model. *New Phytologist* **166,** 791-800.

Piegl L, Tiller W (1997) 'The NURBS book, 2nd ed.' (Springer: New-York)

Planchais I, Sinoquet H (1998) Foliage determinants of light interception in sunny and shaded branches of Fagus sylvatica. L. *Agricultural and Forest Meteorology* **89**, 241–253.

Polhemus Inc. (1993) '3SPACE FASTRAK User's Manual, Revision F.' (Polhemus Inc.: Colchester, VT)

Prusinkiewicz P, Lindenmayer A (1990) 'The Algorithmic Beauty of Plants.' (Springer-Verlag: New York)

Rakocevic M, Sinoquet H, Christophe A, Varlet-Grancher C (2000) Assessing the geometric structure of a white clover (Trifolium repens) canopy using 3-D digitising. *Annals of Botany* **86**, 519-526.

Rice SK, Gutman C, Krouglicof N (2005) Laser scanning reveals bryophyte canopy structure. *New Physiologist* **166**, 695-704.

Sinoquet H, Rivet P (1997) Measurement and visualisation of the architecture of an adult tree based on a three-dimensional digitising device. *Trees: Structure and Function* **11**, 265-270.

Sinoquet H, Thanisawanyangkura S, Mabrouk H, Kasemsap P (1998) Characterization of the light environment in canopies using 3D digitising and image processing. *Annals of Botany* **82**, 203–212.

Sonohat G, Sinoquet H, Kulandaivelu V, Combes D, Lescourret F (2006) Three-dimensional reconstruction of partially 3D digitised peach tree canopies. *Tree Physiology* **26**, 337-351.

Tanaka T, Yamaguchi J, Takeda Y (1998) Measurement of forest canopy structure with a laser plane range-finding method - development of a measurement system and applications to real forests. *Agricultural and Forest Meteorology* **91**, 149-160.

Weber J, Penn J, (1995) Creation and rendering of realistic trees. SIGGRAPH 95 proceedings, pp. 119-128.

doi : 10.1071/FP08051

515 **Tables**

516 Table 1. Distribution of eleven selected young *Fagus sylvatica* trees in four light classes in
517 forest stands of central France.

| Light class | Class bounds (%light) | Number of trees |
|---|---|---|
| 1 | 1 – 5% | 4 |
| 2 | 7 – 15 % | 3 |
| 3 | 30 – 40% | 3 |
| 4 | 100% | 1 |

518

doi : 10.1071/FP08051

519 Table 2. *Fagus sylvatica* leaf morphology parameters per light class, and significance of
520 differences between light classes (P < 0.001 ***, P < 0.01 **, P < 0.05 *, and P > 0.05 Ns).

| **Parameters** | | **Light class** | | | | **P** |
|---|---|---|---|---|---|---|
| | | **1-5%** | **7-15%** | **30-40%** | **100%** | |
| **Leaf area A** ($mm^2$) | | 1398 | 1412 | 1380 | 2258 | Ns |
| **Midrib length L** (mm) | | 55 | 54 | 55 | 65 | Ns |
| **Leaf width W** (mm) | | 35 | 36 | 34 | 47 | Ns |
| **W/L** | | 0.63 | 0.68 | 0.64 | 0.72 | Ns |
| **Midrib curvature C** ($mm^{-1}$) | **mean** | 0.01 | 0.02 | 0.02 | 0.02 | Ns |
| | **max** | 0.05 | 0.06 | 0.06 | 0.06 | Ns |
| | **min** | -0.01 | -0.01 | -0.02 | -0.02 | Ns |
| **Openess angle O** (°) | **mean** | 164.0 | 165.9 | 163.6 | 148.5 | Ns |
| | **max** | 174.7 | 176.8 | 176.8 | 174.3 | Ns |
| | **min** | 150.2 | 150.2 | 146.3 | 113.3 | ** |
| **Lamina twirl T** (°) | **mean** | 8.3 | 8.5 | 14.2 | 14.4 | * |
| | **max** | 18.0 | 17.9 | 35.3 | 41.5 | * |
| | **min** | 3.9 | 3.9 | 4.5 | 3.5 | Ns |
| **Allometric coefficient K** | **K** | 0.70 | 0.71 | 0.70 | 0.74 | * |
| | **Kdist** | 0.65 | 0.68 | 0.66 | 0.71 | Ns |
| | **Kprox** | 0.74 | 0.75 | 0.76 | 0.74 | Ns |
| **Transversal curvature TC** (°) | **mean** | 170.1 | 174.3 | 170.0 | 167.5 | Ns |
| | **max** | 179.1 | 179.2 | 179.1 | 178.3 | Ns |
| | **min** | 152.6 | 154.7 | 144.5 | 135.7 | * |
| **Symmetry S** | **mean** | 0.49 | 0.52 | 0.50 | 0.52 | Ns |
| | **max** | 0.55 | 0.59 | 0.55 | 0.55 | Ns |
| | **min** | 0.42 | 0.44 | 0.41 | 0.42 | Ns |

doi : 10.1071/FP08051


**Fig. 1.** Illustration of two digitizing methods: a) Leaf digitizing in a tree with a hand-held electromagnetic digitizer 3Space Fastrack Polhemus; the pointer is set parallel to the midrib and the mean plane of the lamina and points the junction between petiole and lamina. b) Leaf digitizing with a non-contact laser scan digitizer Konica Vi-910 on detached leaves. The light red triangle mimics the emitted laser plane.

doi : 10.1071/FP08051

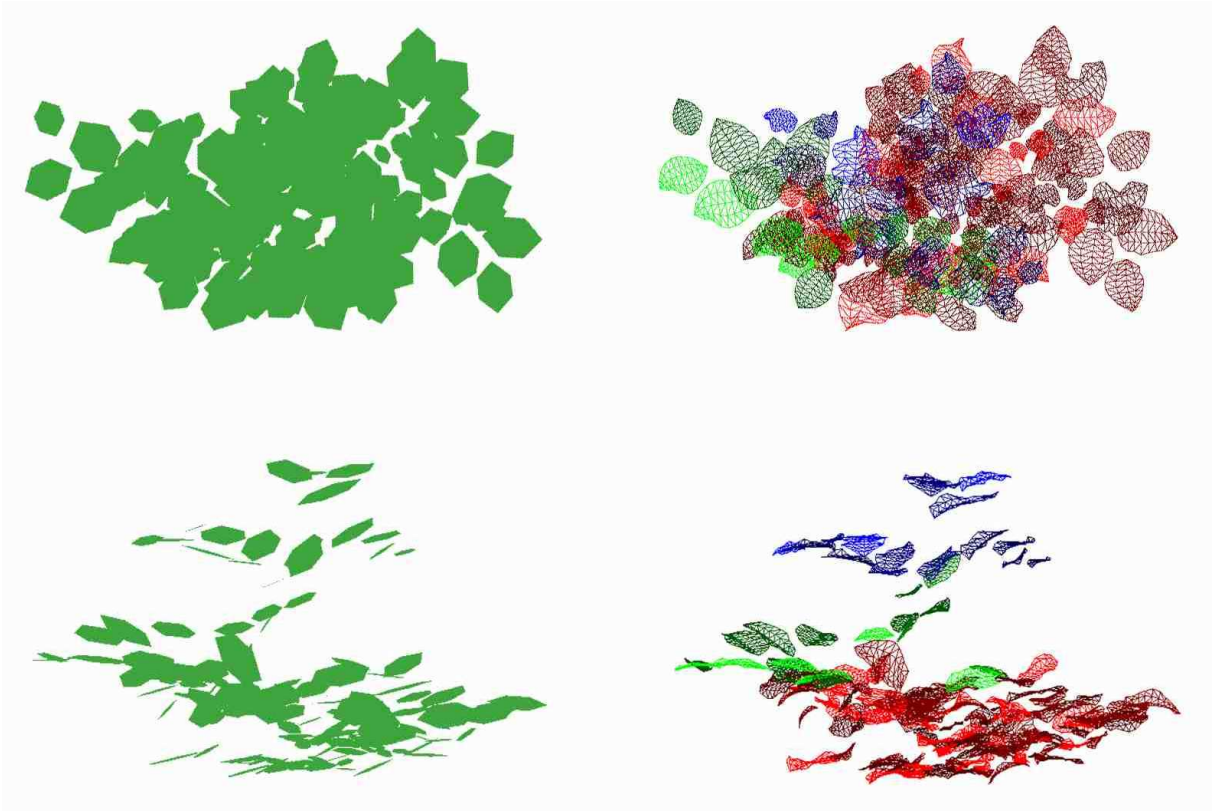

a) b)

**Fig. 2.** Images of three-dimensional plant mock-ups of the same tree (*Fagus sylvatica*) at 9% light viewed from the top (first line) or laterally (second line). a) Three-dimensional mock-up made of planar hexagonal leaves. b) Three-dimensional mock-up made of non-planar triangulated leaves. Blue, green and red false colours are assigned to non-planar leaves in top, medium and bottom canopy layers.

doi : 10.1071/FP08051

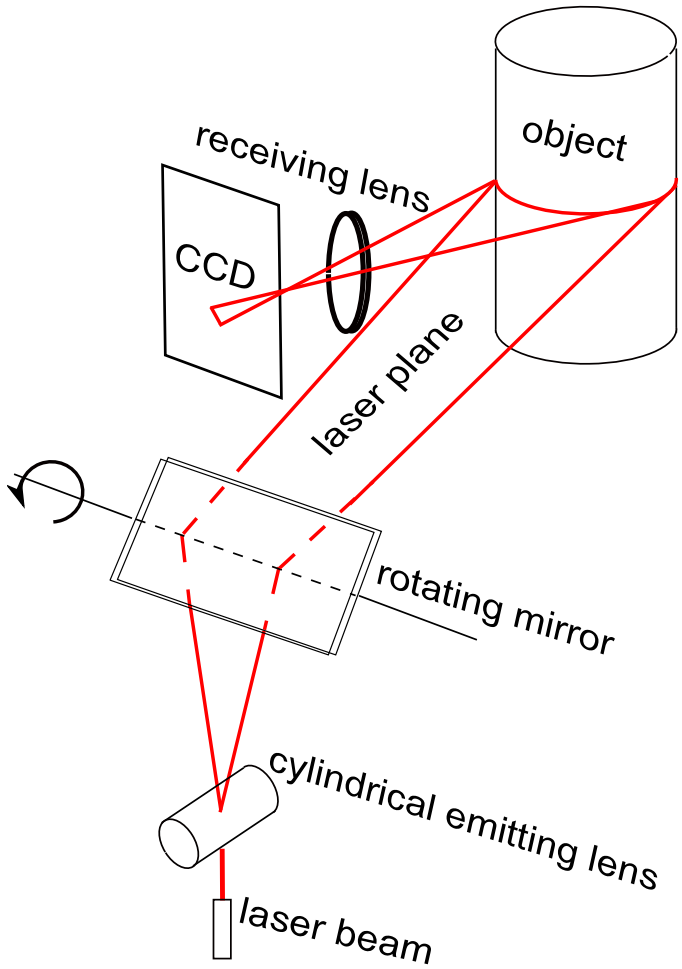


**Fig. 3.** Illustration of the light stripe method used in the Konica Vi-910 scanner: a red laser beam is emitted through a cylindrical lens in order to generate a laser plane. The laser plane is sent to a rotating mirror in order to scan the object. Reflected light by the object is converted into distance information by using an active triangulation principle. The conversion is achieved through a charge-coupled device camera.

doi : 10.1071/FP08051

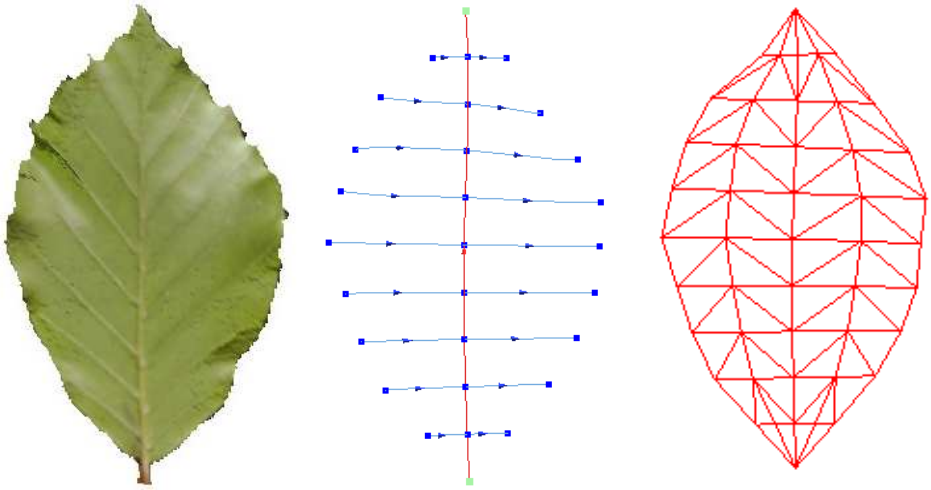

a) b) c)

**Fig. 4.** Processing of the three-dimensional leaf point cloud acquired with a non-contact laser scan digitizer (Konica Vi-910) to extract morphological parameters and obtain a non-planar leaf model made of 72 triangles: a) Scanned *Fagus sylvatica* leaf made of 18927 coloured points; b) Nine slicing NURBS (Non Uniform Rational B-Spline) curves devoted to the extraction of leaf morphological parameters and the construction of a triangulated leaf model; c) Resulting triangulated leaf model composed of 72 triangles.

doi : 10.1071/FP08051

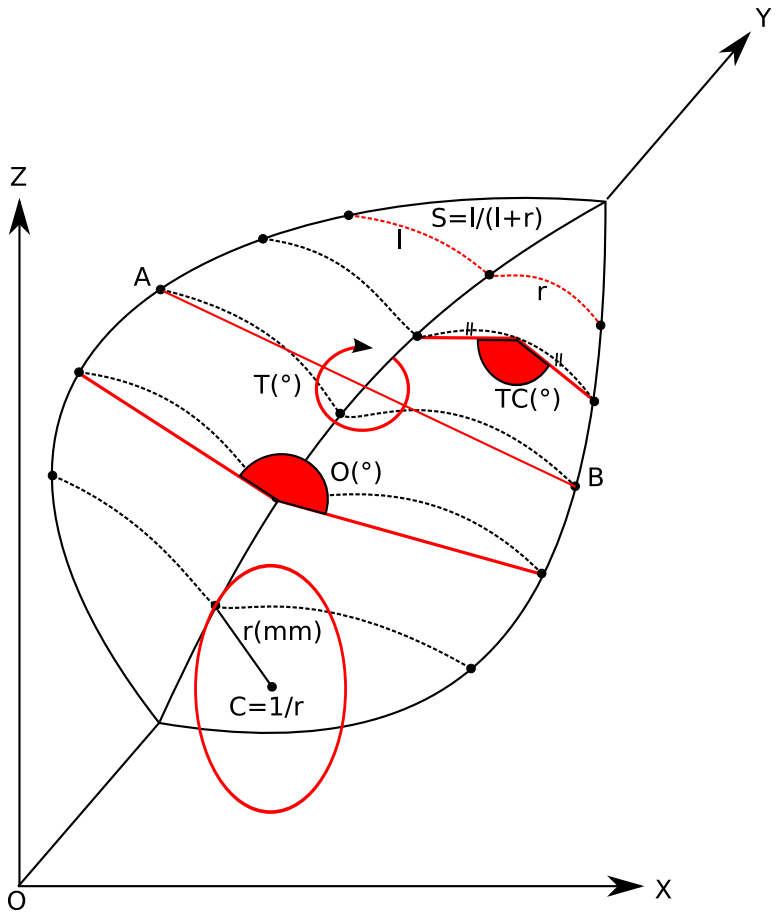


**Fig. 5.** Illustration of five morphological parameters of a *Fagus sylvatica* leaf, namely midrib curvature C, openness angle between two-half laminas O, lamina twirl T, transversal curvature angle of lamina TC and symmetry between the two half-laminas S. First slicing curve, illustration of C ($mm^{-1}$) i.e. the inverse of the osculating circle radius; second slicing curve, O (°); third slicing curve, T (°), defined as the rotation angle of the segment AB around the Y axe; fourth slicing curve, TC (°); fifth slicing curve, S.

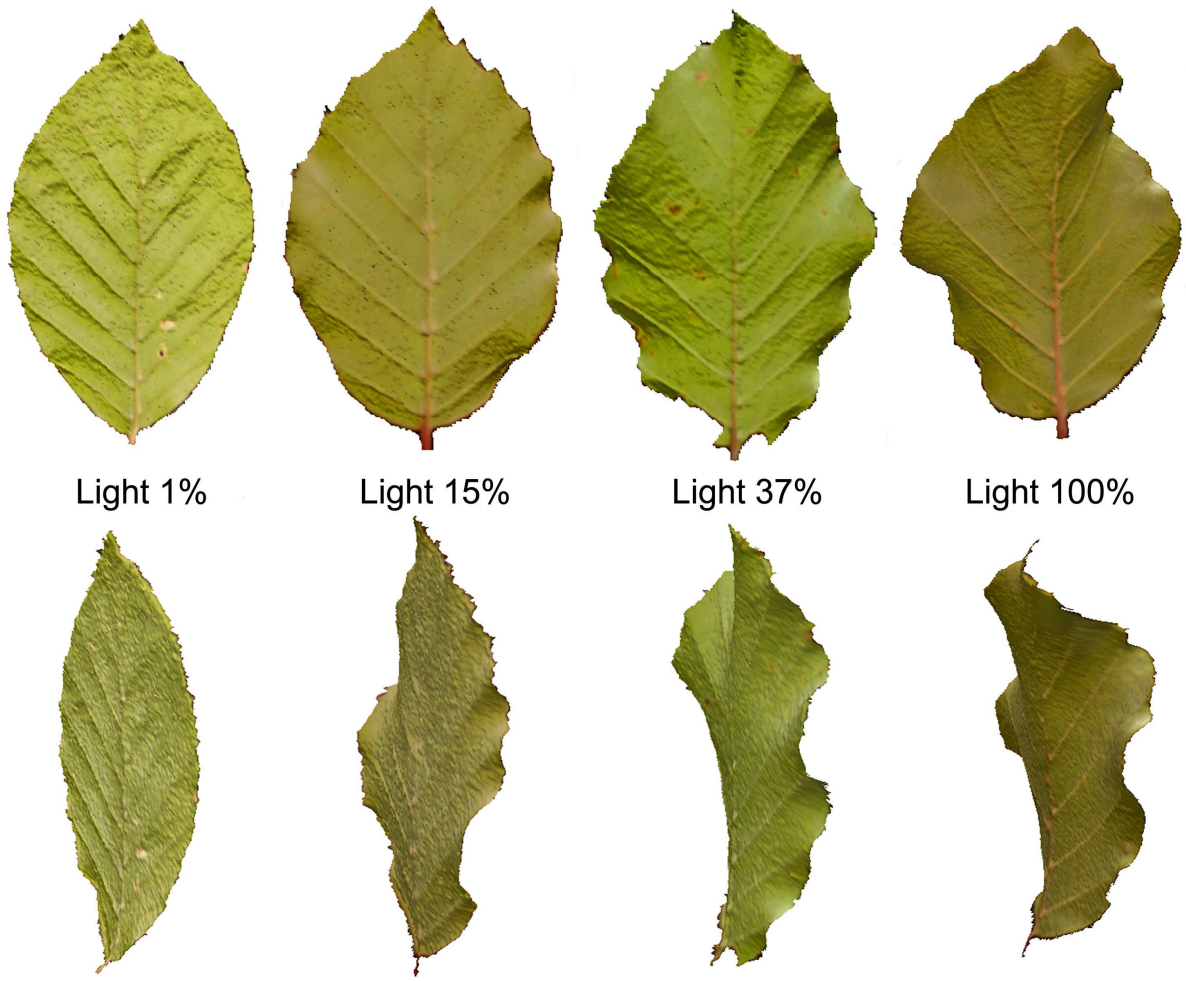


**Fig. 6.** *Fagus sylvatica* leaves as a point cloud originated from the laser scanner (Konica Vi-910) for some young trees sampled under different light availabilities. Top panel: perpendicular view to the main leaf plane. Bottom panel: parallel view to the main leaf plane

doi : 10.1071/FP08051

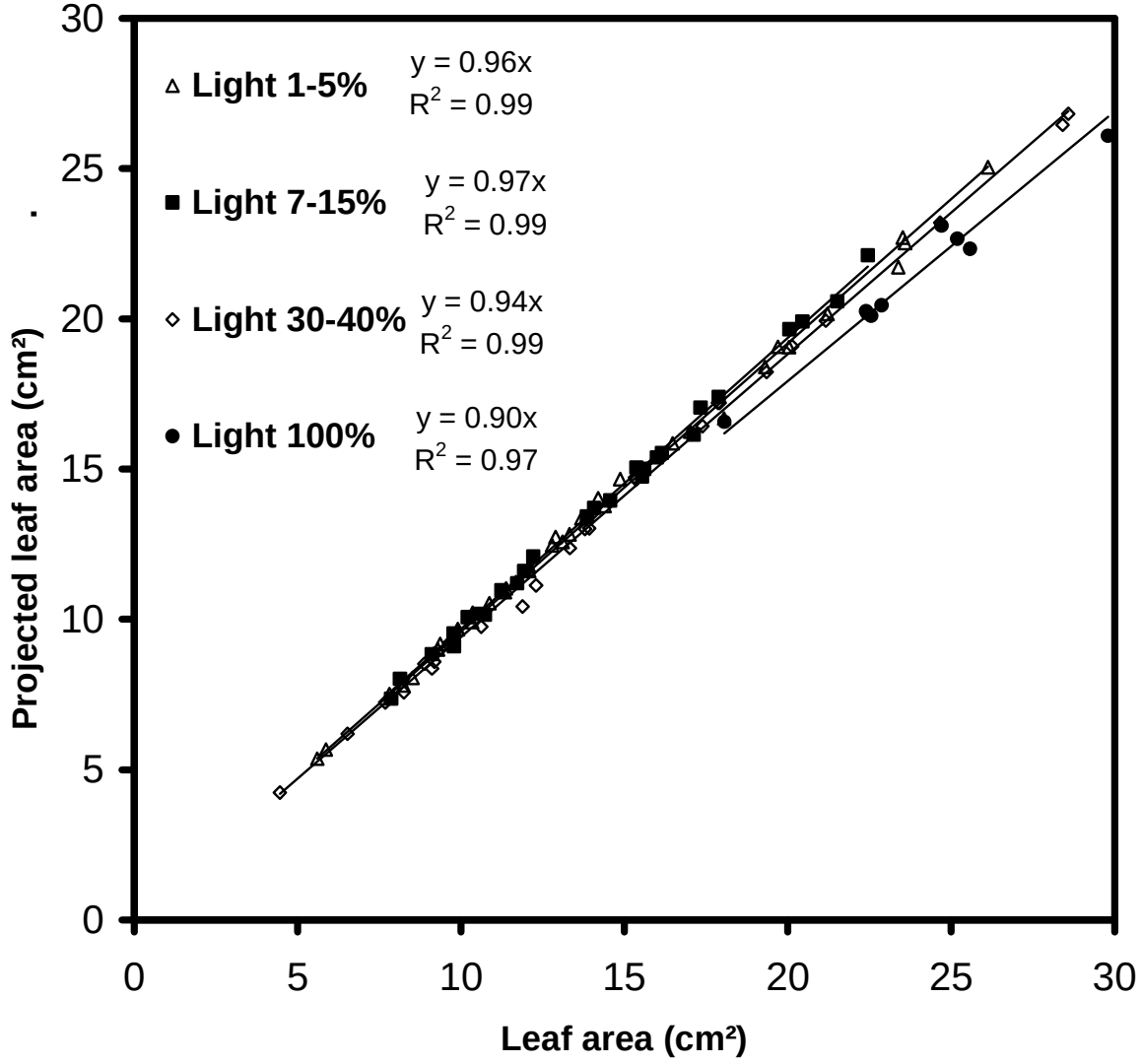


563

564 **Fig. 7.** Silhouette to total leaf area ratio integrated on the whole sky, $STAR_{SKY}$, of individual
565 non-planar leaves of *Fagus sylvatica* in central France under different light availabilities,
566 shown as a scatter plot between individual leaf area and projected leaf area averaged over all
567 sky directions.

doi : 10.1071/FP08051

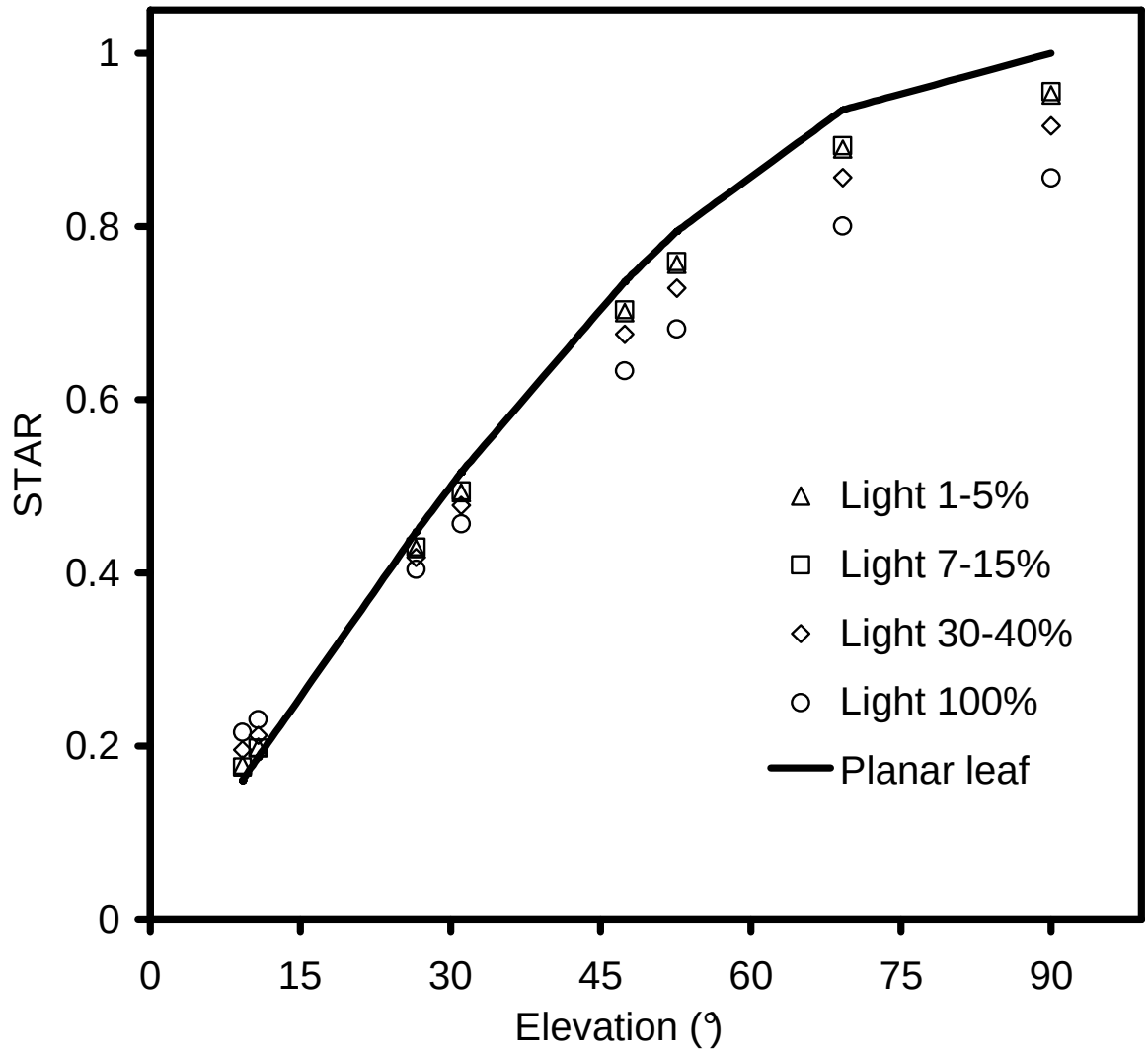


568

569 **Fig. 8.** Directional STAR (Silhouette to Total leaf Area ratio) as a function of elevation angle
570 of individual non-planar leaves of *Fagus sylvatica* under different light availabilities in
571 Central France and in comparison with planar leaves (dark line).

572

doi : 10.1071/FP08051

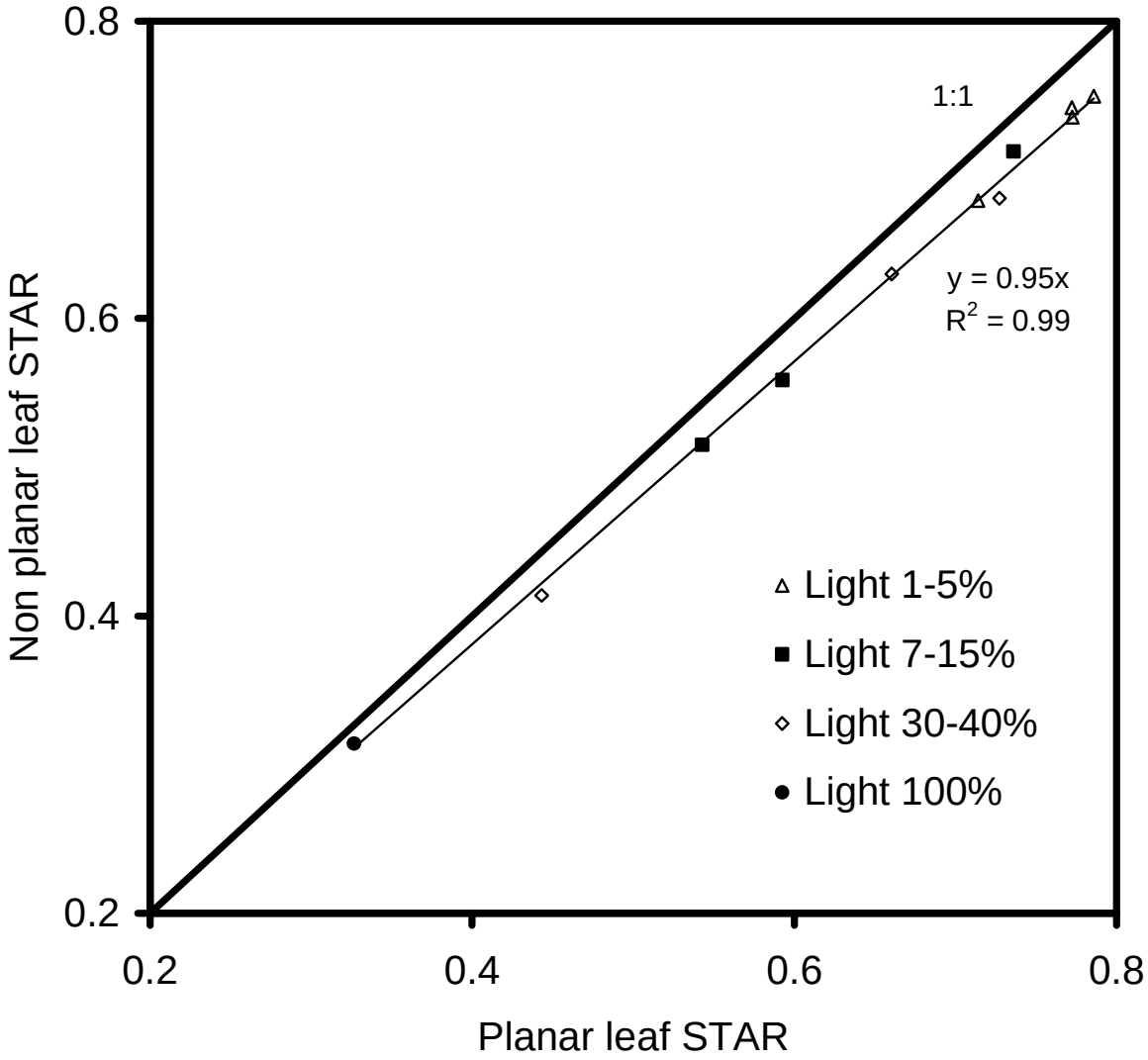


573

574 **Fig. 9.** Comparison between silhouette to total leaf area ratio integrated on the whole sky
575 ($STAR_{SKY}$) of *Fagus Sylvatica* trees under different light availabilities in central France
576 calculated on mock-ups with planar and non-planar leaves.

577

doi : 10.1071/FP08051

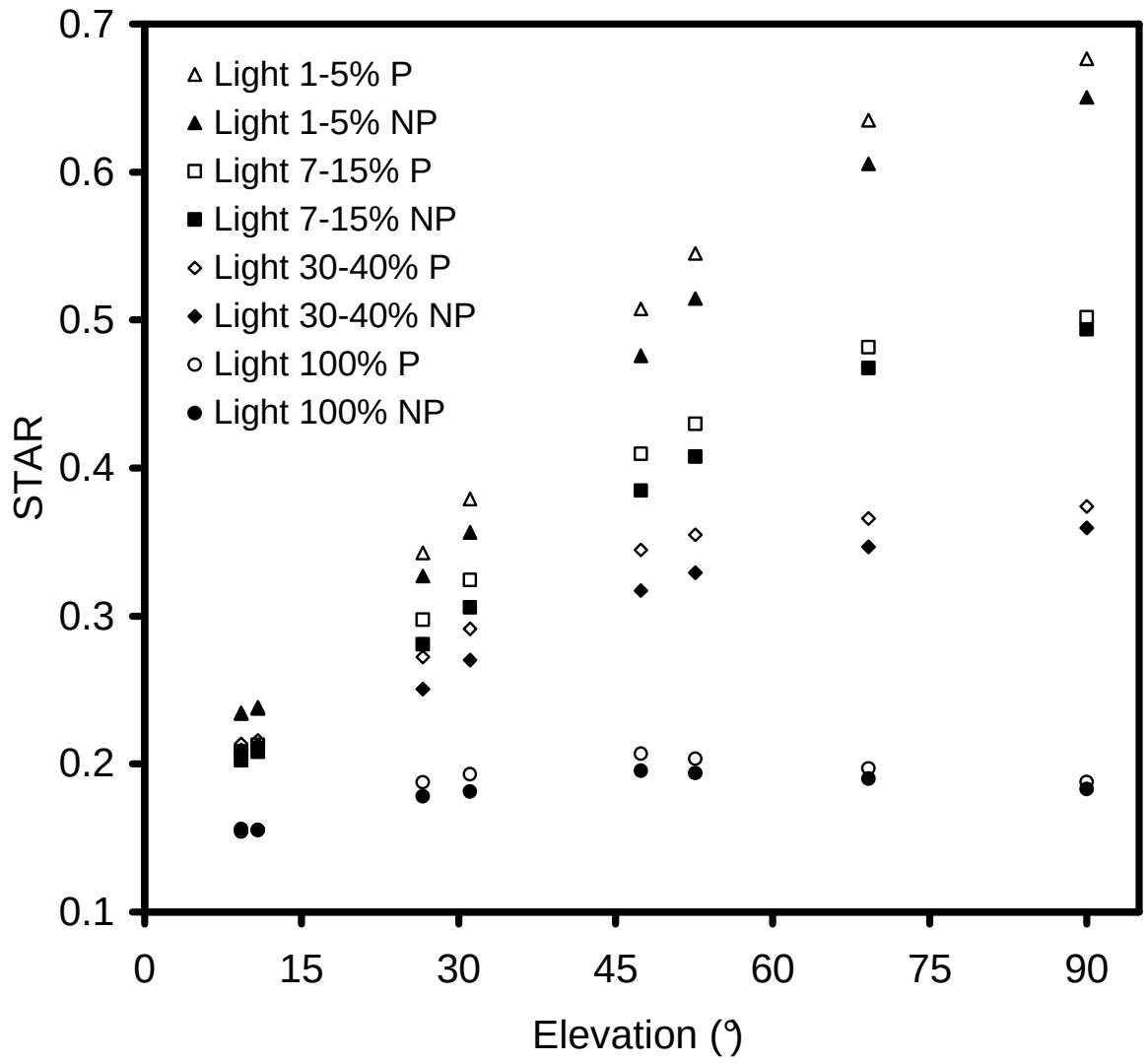


578

579 **Fig. 10.** Directional silhouette to total leaf area ration (STAR) as a function of elevation angle
580 of *Fagus Sylvatica* trees under different light availabilities in central France calculated on
581 mock-ups with planar (P) and non-planar (NP) leaves.